Stability Analysis of Rainfall Induced Landslide

THESIS SUBMITTED IN PARTIAL FULFILLMENT OF THE REQUIREMENTS FOR THE DEGREE
Of
MASTER OF CIVIL ENGINEERING
Specialization In
SOIL MECHANICS AND FOUNDATION ENGINEERING (SMFE)

By
SAYAN CHANAK
(*Class Roll No.- 002210402011*)

UNDER THE GUIDANCE OF
Dr. GUPINATH BHANDARI
Associate Professor, Department of Civil Engineering
Jadavpur University

DEPARTMENT OF CIVIL ENGINEERING
JADAVPUR UNIVERSITY
KOLKATA 700032

June 2024

DEPARTMENT OF CIVIL ENGINEERING
JADAVPUR UNIVERSITY

DECLARATION

I hereby declare that this thesis contains literature survey and original research works by the undersigned candidate, as part of my Master of Civil Engineering in Soil Mechanics & Foundation Engineering studies. All the information in this document have been obtained and presented in accordance with academic rules and ethical conduct. I also declare that, as required by these rules and conduct, I have fully cited and referenced all material and results that are not original to this work.

Name	Sayan Chanak
Class Roll No.	002210402011
Eamination Roll No.	M4CIV24009
Registration No.	144004 of 2018-19
Thesis Title	***Stability Analysis of Rainfall Induced Landslide***
Institution Name	Department of Civil Engineering, Jadavpur University
Signature	
Date	
Place	Jadavpur, Kolkata 700032

DEPARTMENT OF CIVIL ENGINEERING
JADAVPUR UNIVERSITY

CERTIFICATE OF RECOMMENDATION

I hereby recommend that the thesis prepared under my supervision by **Sayan Chanak** entitled "***Stability Analysis of Rainfall Induced Landslide***" be accepted in partial fulfilment of the requirements for the Degree of *Master of Civil Engineering* with specialization in *Soil Mechanics and Foundation Engineering* from Jadavpur University during the year 2023-2024.

Dr . Gupinath Bhandari

In-Charge of thesis
Associate Professor,
Department of Civil Engineering
Jadavpur University , Kolkata

Prof. Partha Bhattacharya

Head of Department
Departnent of Civil Engineering
Jadavpur University , Kolkata

Prof . Dipak Laha

Dean
Faculty of Engineering &Technology
Jadavpur University , Kolkata

DEPARTMENT OF CIVIL ENGINEERING
JADAVPUR UNIVERSITY

CERTIFICATE OF APPROVAL

The foregoing thesis titled **"*Stability Analysis of Rainfall Induced Landslide*"** is hereby approved as a creditable study for an Engineering subject carried out and presented in a manner satisfactory to warrant its acceptance as a pre- requisite to the degree for which it has been submitted. It is understood that by this approval the undersigned do not necessarily endorse or approve any statement made, opinion expressed or conclusion drawn therein, but approve this thesis only for the purpose for which it is submitted.

Committee in final evaluation of the Thesis

(Signature of External Examiner)

(Signature of Thesis Supervisor)

ACKNOWLEDGEMENT

The success and final outcome of this Work required a lot of guidance and assistance from many people and I am extremely fortunate to have got this all along the completion of my thesis work. Whatever I have done is only due to such guidance and assistance and I would not forget to thank them. I respect and thank my guide Dr. Gupinath Bhandari, for giving me an opportunity to do the thesis work on slope instability analysis due to rainfall and providing me all support and guidance which made me complete the project on time, also I would like to thank Joyita Golder, PhD scholar under Prof. Gupinath Bhandari for guiding me in this project.

I am extremely grateful to all the faculties for providing such a nice support and guidance.

I also acknowledge the cooperation and assistance provided by my classmates and my family members during this work.

Sayan Chanak
(***Roll No. - 002210402011***)

M.C.E., 2nd Year , Final Semester
Jadavpur University , Kolkata-32

CONTENTS

List of Tables

List of Figures

Abstract

Landslides represent one of the most common natural disasters globally. A landslide occurs when the stability of a slope is disrupted, often due to heavy rainfall, earthquakes, volcanic activity, or human activities like deforestation or construction. This disruption causes the soil and rock on the slope to lose cohesion and slide downhill. Rainfall-induced landslides can have devastating effects for the environment and human populations. While landslide-prone areas often experience recurrent occurrences, landslides can also occur in previously unaffected regions. In the current study, a new landslide was observed in March 2022 at Pangthang, East Sikkim. The study focused on a landslide in hilly terrain, collecting subsoil data and analyzing factors contributing to landslides. Using PLAXIS 2D software, stability analysis of the slope was conducted. Before construction, the slope was stable under fair weather conditions with a Factor of Safety of 1.331. After construction, including surcharge loads from superstructures, the slope remained stable under fair weather conditions with a Factor of Safety of 1.284. After heavy precipitation, landslides occurred exposing the foundation of a building. A nearby Jhora, and the middle of the slope adjacent to it, experienced failure. Considering the impact of a high infiltration rate of 0.12m/h, stability analysis using PLAXIS 2D software yielded a Factor of Safety of 0.95. To address the issue, an effective and affordable remedial measure was pursued. A sand drain was proposed to mitigate pore water pressure by capturing subsurface water and draining it from the bottom of the slope. Additionally, the slope was reinforced using concrete piles to enhance the shear strength of the weaker soil mass.

CHAPTER : 1

INTRODUCTION

1.1 General

Movement of soil mass in the downward direction, either in case of natural or manmade slopes, is termed as landslides. Landslides and slope failures are two of the most common catastrophic natural disasters worldwide. Landslides can be triggered by a range of factors, such as seismic activity, erosion of slopes, adding excessive weight, and inadequate surface or underground drainage systems. They can result from natural processes, human activities, and shifts in climate patterns. Climate change has led to alterations in the natural hydrological system, as noted by the IPCC in 2007, contributing to landslides in mountainous regions. While landslide-prone areas can typically be identified by recurrent occurrences, new landslides may also emerge in previously unaffected areas, possibly as a result of climate change. For instance, the landslide in Mirik in July 2015 serves as an illustration of a fresh landslide event.From a theoretical and practical standpoint, the topic of stability analysis of rain-induced soil failures is fascinating, significant, and challenging in the field of geotechnical engineering. Because of geology and hydrogeologic processes, hillslopes can become mechanically unstable, resulting in slope failures and landslides that pose a major risk to human life and built environments both and close to downward mass movement. These slope failures are now frequent geotechnical issues, with Hong Kong, Italy, Singapore, and India having the highest rates of occurrence.

In the northern Indian Himalayan region, slope failures leading to landslides are a very common natural hazard. These failures can occur due to various factors such as geological conditions,hydrological condition, weathering, seismic activity, and human interventions like deforestation or construction activities. The region's steep terrain, high rainfall, and seismic vulnerability exacerbate the risk of slope failures. The geological composition, including weak rock formations and loose sedimentary layers, contributes to the instability of slopes.Climate

change-induced changes in precipitation patterns and increasing extreme weather events also play a role in triggering landslides. Intense rainfall can saturate the soil, reducing its stability and leading to slope failures. Additionally, human activities like deforestation, road construction, and urbanization can disturb the natural balance of the terrain, making slopes more susceptible to failure. The consequences of slope failures in the northern Indian Himalayan region can be severe, including loss of life, damage to infrastructure, disruption of transportation networks, and environmental degradation. One significant example of slope failure in the northern Indian Himalayan region is the Uttarakhand flash floods of 2013. While not solely caused by slope failure, the event involved massive landslides triggered by heavy rainfall, which led to devastating flash floods. The steep slopes and fragile geological formations in the region contributed to the severity of the landslides, exacerbating the impact on communities, infrastructure, and the environment.Another notable example is the Malpa landslide disaster of 1998 in the Kali River valley of Uttarakhand. This catastrophic event was triggered by heavy rainfall and involved multiple landslides, which blocked the flow of the river, resulting in the formation of a temporary lake. Subsequent breaching of the debris dam caused flash floods downstream, leading to significant loss of life and property.In addition, the Leh flash floods of 2010 in Ladakh, though not in the traditional northern Indian Himalayan region, demonstrated the vulnerability of mountainous areas to slope failures. Cloudburst-triggered landslides caused flash floods, devastating the town of Leh and surrounding areas, highlighting the risks associated with steep terrain and intense rainfall events in such regions.

Rainfall events in northern India are becoming increasingly frequent and strong due to climate change. Severe precipitation events lead to landslides, flash floods, and soil erosion, which disrupt livelihoods, cause fatalities, and damage infrastructure. According to **Crozier** (2010), there are three main hydrological elements related to climate change affecting the frequency of landslides. These factors include increased wind speeds, rising temperatures, and prolonged, heavy rains. Increases in total precipitation lead the soil's capillary suction to decrease, which decreases the soil's effective stress. Rainfall can raise the water table, reducing the soil's shear strength and increasing its bulk density. These changes in soil characteristics brought on by increased precipitation increase the risk of landslides.

Sikkim, located in the northeastern part of India, experiences diverse rainfall patterns influenced by its topography, elevation, and proximity to the Bay of Bengal. Like much of India, Sikkim's rainfall is heavily influenced by the Indian monsoon. The south west monsoon,

which typically arrives in June and lasts until September, brings the majority of the annual rainfall to the region. Because of Sikkim's diverse topography, which ranges from alpine meadows to subtropical lowlands, there are notable differences in rainfall in different areas and at different elevations. The orographic effect and closeness to the Bay of Bengal cause the southern and central sections of Sikkim—including places like Gangtok and Namchi—to receive more rainfall than the northern districts. The steep slopes of the Himalayas play a crucial role in enhancing rainfall in Sikkim through orographic lifting. As moist air masses from the Bay of Bengal encounter the Himalayan barrier, they are forced to rise, cool, and condense, leading to enhanced precipitation on the windward side (southern and eastern slopes) of the mountains. The distribution of rainfall in Sikkim demonstrates both temporal and spatial variability. Rainfall in the state's southern and eastern regions, including areas like Gangtok, is comparatively greater and frequently exceeds 3,000 mm per year. In comparison, there is less rainfall in the northern and western regions, and certain areas even experience semi-arid conditions. Sikkim experiences distinct seasonal patterns of rainfall. The southwest monsoon brings the primary rainy season from June to September, accounting for the bulk of the annual precipitation. The post-monsoon period (October to November) and pre-monsoon period (April to May) also witness some rainfall, albeit lesser in intensity.

In Sikkim's valleys and foothills, alluvial soils are common. These soil types are created when sediments are deposited by rivers and streams. The upper altitudes of Sikkim are dominated by mountain soils, which are distinguished by their rocky landscape, shallow depth, and sparse population. Because of their steep slopes, erosion, and scant vegetation, these soils frequently show poor fertility and drainage. Sikkim's vast forest cover helps to create rich, organically-rich forest soils that are home to a variety of plants. Glacial soils are common in Sikkim's glaciated regions, such as the high-altitude highlands with year-round snow and ice. Typically, glacial till, moraine deposits, and other unconsolidated sediments make up these soils. Gravitational processes cause rock pieces, debris, and soil particles to accumulate near the base of slopes, resulting in colluvial soils. Because of the local geology and slope shape, these soils frequently have high shear strength, varied composition, and heterogeneous characteristics. In certain parts of Sikkim, weathering processes have changed the underlying rock formations, resulting in lateralitic soils, which are distinguished by its reddish hue and iron-rich content. These soils have characteristics including low bearing capacity, high flexibility, and erosion vulnerability.

1.2 Motivation

Rainfall-induced landslides can have devastating effects for the environment and human populations. People can be buried behind debris during landslides, which can result in significant casualties. Fast-moving landslides have the potential to be especially lethal since they can happen suddenly. Houses, structures, and infrastructure such as utilities, roads, and bridges can all be completely destroyed or seriously damaged. Communities can be devastated by a landslide's destructive power, which can destroy buildings.The expense of repairing and rebuilding after property and infrastructure are destroyed is substantial. Both local and national economies may be impacted by disruptions to economic activity, especially if vital infrastructure like electricity lines or highways is damaged.

In 2023, **Joyita et al. [1]** investigated a landslide that occurred in March 2022 at Pangthang, East Sikkim. The location in question was assessed for landslide susceptibility using geospatial technology analysis, ground surveying, and soil investigation; the results showed that the area was not susceptible to landslides; yet, a continuous, intense, unexpected rainfall preceded the landslide. They analyzed the slope before and after implementing remedial measures to account for the impact of climate change, particularly heavy precipitation, using the Bishop Method **[2]**.They found that under fair weather conditions, the Factor of Safety (FoS) exceeded 1.3, specifically reaching 1.39, indicating that the slope is stable. However, when higher precipitation was considered, the FoS decreased to 0.93, leading to slope failure in the field. They pointed out the significance porewater pressure was in triggering the collapse. They proposed an eco-friendly and low-cost remedial measure to address the issue. To reduce pore water pressure, a sand drain was suggested to capture subsurface water and channel it out through the bottom of the slope. The slope surface was prepared and seeded with vetiver grass, and a layer of jute geotextile was applied to prevent surface erosion. Additionally, the slope was reinforced using Sal-Bullah, an indigenous technology and material, which helped to subdivide the slope height and reduce the surcharge load. After implementing the remedial measures, they found that the slope appeared stable, with the Factor of Safety increasing to 1.48.

Traditionally, slope stability analysis has been conducted using the limit equilibrium approach. However, in recent years, the finite element/finite difference method with the shear strength reduction (SSR) technique has gained popularity for practical slope stability analysis **[3][4][5]**. Research has demonstrated that the SSR technique is a reliable and robust approach for assessing the safety factor of slopes and identifying critical slip surfaces. One of the key advantages of the SSR technique is its automatic determination of failure surfaces within the material, where shear stresses exceed the shear strength. Unlike traditional methods that rely on slice assumptions, the SSR technique eliminates the need for assumptions about inter-slice side forces.

Chatra et al. in 2017 **[6]** utilized FLAC to investigate slope instability induced by rainfall. Their analysis involved transient flow analysis to determine pore-water pressures necessary for evaluating the shear strength of unsaturated soils. Subsequently, to achieve a state of limiting equilibrium, they conducted Factor of Safety (FOS) calculations employing the Shear Strength Reduction (SSR) technique, progressively reducing the material's shear strength (cohesion and friction). Numerous researchers have employed finite element software such as ABAQUS or ANSYS to investigate slope stability and simulate disasters. Onyango et al. **[7]** investigated the stability of the slope supporting the Qinglong-Xingyi Expressway Contract Section and proposed an appropriate stabilization method. They developed a 2D simulation model of the slope using Finite Element Software ANSYS for analysis. The findings of their research contribute to enhancing numerical analysis through strength reduction as a decision-making tool for addressing slope stability issues. **Jacob et al.** in 2018 **[8]** conducted an analysis of both failed and existing slopes. The study involved examining slope failures or investigating landslides to determine the causes of failure and recommend potential remedial measures. Additionally, stability assessments were performed on existing slopes, followed by calculations of the factor of safety and failure slip circle using Plaxis (2D).

1.3 Objective

This study aims to achieve a comprehensive understanding of the slope failure due to rainfall infiltration into soil slope and failure of unsaturated soil slope using finite element based PLAXIS 2D software. The primary objectives are as follows:

1) To evaluate the factor of safety of concerned slope with and without considering the effect of precipitation and to find the actual cause of failure.
2) To offer a practical and cost-effective solution.

CHAPTER : 2

LITERATURE SURVEY

2.1 General

Numerous research studies have focused on exploring rainwater infiltration into slopes and assessing slope stability during rainfall events. Infiltration is a critical factor influencing slope stability during rainfall. This chapter presents a brief overview of the current body of research in these areas. Recent advancements in analyzing slope stability under rainfall conditions are outlined. Additionally, significant findings from existing research regarding critical factors associated with rain-induced landslides are summarized and discussed.

Wu et al. (2015) **[9]** conducted a series of physical tests aimed at simulating slope failures induced by rainfall. The experiments explored two scenarios: rainwater infiltration into the slope and slope failures triggered by artificial rainfall under various initial conditions. Observations were made on slope deformation and failures, and potential mechanisms were interpreted based on the experimental results. Their findings confirmed the hypothesis that pore-water pressure and water content in a loose soil slope undergo rapid changes, with water infiltration into cracks significantly impacting landslide development. The observed slope failures were categorized into three types: overall sliding failure, partial sliding failure, and flow slide. **Prodan et al**. (2023) **[10]** analyzed landslide initiation caused by artificial rainfall by small-scale slope modeling. They maintained constant slope angles while using a 2.3 x 1.0 x 0.5 m platform with different types of soil, such as sand and sand-kaolin mixtures. At various depths and profiles, they observed hydraulic reactions such as water content, pore pressure, and suction. It addresses the variables that affect the beginning and spread of landslides, emphasizing the importance of soil type, infiltration, and general soil resistance, which includes variables like matric suction and soil strength. Their findings show that rainfall causes slope failure by increasing water content, decreasing suction, and weakening the soil. While sand-kaolin combinations exhibit instabilities through crack formation due to suction dissipation,

sand slopes fail as a result of groundwater rising. The study conducted by **Fayaz et al.** (2022) **[11]** offers scientific insights into monitoring, prevention, and early warning systems for rainfall-induced landslides. In this research, a physical model test on rainfall-induced landslides was performed using a self-made artificial rainfall system. Soil materials were simulated based on martial similarity theory from the study site located on Sadhna Road in Kupwara, Jammu and Kashmir, known for its history of continuous slope failure. The methods employed proved effective in monitoring pore water infiltration and studying the sliding mechanism and factors inducing slope failure. Rainfall intensity was recorded at 295 mm/hr, with 10mm depth introduced per session. Surface erosion was observed to be more prevalent initially than internal landslide movement. The primary factor contributing to shallow landslides on the Sadna slope was identified as high rainfall. Researchers also conducted centrifuge modeling to analyze slope stability. **Wang et al**. (2021) **[12]** conducted centrifuge tests to investigate rainfall-induced instabilities in variably saturated slopes. They examined the effects of rainfall intensity and initial conditions such as slope angle, porosity, and soil saturation on failure initiation and post-failure kinematics. Two main failure modes were identified: slide-to-flow and flowslide. Slide-to-flow involves soil mass flow along a continuous shear surface after initial failure, while flowslide is characterized by rapid surface erosion channels followed by soil mass acceleration. Flowslide typically produces multiple superficial shear surfaces and longer run-out distances. Rainfall intensity and saturation profiles are crucial in both failure initiation and post-failure soil mobilization stages.

2.2 Mechanics of un-saturated soil

Unsaturated soil mechanics is a branch of soil mechanics that focuses on the behavior and properties of soils that are not fully saturated with water. Unlike saturated soils, which have all their pore spaces filled with water, unsaturated soils contain both water and air in their pores. This condition significantly affects the soil's mechanical properties and behavior, making the study of unsaturated soils essential for various engineering applications, including slope stability, foundation design, and environmental engineering. Unsaturated soil mechanics helps in understanding the stability of slopes, especially in partially saturated conditions where matric suction can contribute to apparent cohesion and influence slope stability. Key Concepts in Unsaturated Soil Mechanics are discussed bellow :

- Matric Suction: The difference between pore air pressure and pore water pressure. It is a measure of the water's tendency to move within the soil due to capillary action.

- Soil-Water Characteristic Curve (SWCC):The Soil-Water Characteristic Curve (SWCC) describes the relationship between a soil's water content and matric suction. It is an essential tool for understanding and predicting the hydraulic behavior of unsaturated soils. The curve typically illustrates how soil retains water at various suction levels, highlighting distinct zones for saturation, desaturation, and residual water content.

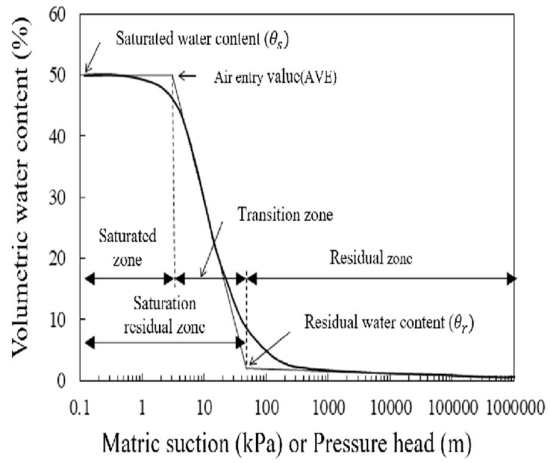

Fig.1 : Soil-water Characteristic-Curve curves

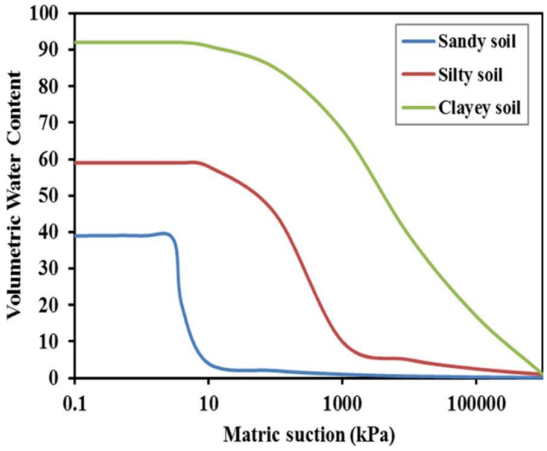

Fig.2 : Typical soil-water-characteristic-for different types of soils (Fredlund and Xing 1996)

- Hydraulic Conductivity Function (HCF): In unsaturated soils, hydraulic conductivity varies with the degree of saturation. As the soil dries, water pathways become more tortuous and less continuous, resulting in reduced hydraulic conductivity. Because direct measurement is time-consuming and costly, the permeability function of unsaturated soil is commonly estimated using the soil-water characteristic curve (SWCC) **[13].**

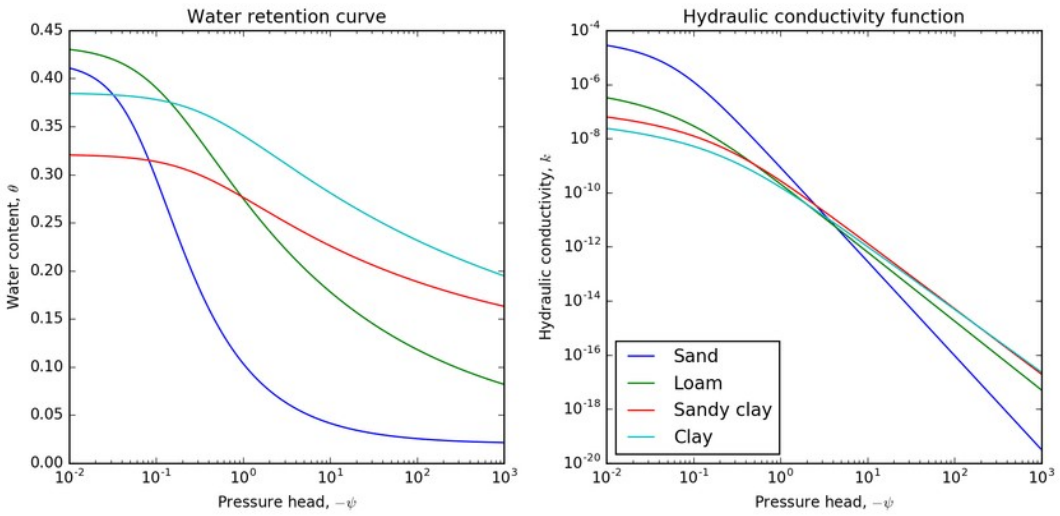

Fig. 3: The water retention curve and the hydraulic conductivity function for four canonical soil types of sand, loam, sandy clay, and clay.(Rowan Cockett 2018)

2.2.1. Shear-Strength of Unsaturated Soil

1) Bishop's effective stress equation : Bishop's effective stress equation **[14]** is often used, which incorporates a parameter (χ) representing the degree of saturation:

$$\sigma' = \sigma - ua + \chi\,(ua - uw)$$

where $\sigma'$is the effective stress, σ is the total stress, ua is the pore air pressure, uw is the pore water pressure, and χ varies between 0 (dry soil) and 1 (fully saturated soil).

2) Fredlund Method (**Fredlund et al.** in 1978**[15]**) : The shear strength (τ) of unsaturated soils can be described by an extended version of the Mohr-Coulomb failure criterion:

$$\tau = c' + \sigma' \tan\phi' + (ua - uw)\tan\phi b$$

where c' is the effective cohesion, ϕ' is the effective angle of internal friction, and ϕb is the angle indicating the rate of increase in shear strength with matric suction.

Fredlund and Xing model (1996) **[16]** describes the relationship between SWCC and shear strength of unsaturated soil.

2.2.2. Flow through Unsaturated soil

Flow through unsaturated soil, often referred to as unsaturated flow, is a critical aspect of unsaturated soil mechanics. This process is complex due to the simultaneous presence of air and water in the soil pores, leading to unique hydraulic properties that differ significantly from those in fully saturated soils. Understanding unsaturated flow is essential for a variety of applications, including irrigation management, slope stability analysis, contaminant transport, and the design of drainage systems.

The primary equation used to model unsaturated flow is Richards' equation, which combines Darcy's law for unsaturated flow with the continuity equation:

$$\partial t/\partial\theta=\partial/\partial z\ [K(\theta)(\partial z/\partial h+1)]$$

where θ is the volumetric water content, t is time, $K(\theta)$ is the hydraulic conductivity as a function of water content, h is the matric suction head, and $z$is the spatial coordinate.

2.3 Numerical Modellings

Researchers have developed various models of rainfall-induced slope stability to simulate field conditions and explore the relationship between rainfall infiltration and slope stability **[17] [18]**. Rainfall infiltration into unsaturated soil is primarily analyzed using transient seepage analysis. Researchers also measured the amount of rainfall that infiltrates the soil slope and the amount that creates surface runof **[19] [20] [21]**. These models aim to provide a comprehensive understanding of how different rainfall patterns and intensities impact slope stability. Subsequently, slope stability analysis is performed using Limit Equilibrium Method (LEM) based software such as SLOPE/W. This software helps determine the Factor of Safety (FOS) by assessing the balance between driving forces (such as gravity) and resisting forces (such as soil strength) on a slope**[17] [20]**. The integration of transient seepage analysis with LEM allows for a more accurate prediction of slope behavior under varying rainfall conditions. Through these studies, researchers can identify critical factors that contribute to slope failures and develop effective mitigation strategies. These strategies may include designing better drainage systems, reinforcing slopes, and implementing early warning systems to reduce the

risk of landslides. By understanding the dynamics of rainfall infiltration and slope stability, these models provide valuable insights for engineers and planners to ensure the safety and stability of slopes in vulnerable regions in world.

2.4 PHI/C Reduction Method

The safety calculation type is an option available in PLAXIS to compute global safety factors. In the safety approach the shear strength parameters **tanϕ** and **C** of the soil are successively reduced until failure of the structure occurs . The total multiplier ΣMsf is used to define the value of the soil strength parameters at a given stage of analysis :

$$\Sigma Msf = \frac{tan\phi_{input}}{tan\phi_{reduced}} = \frac{C_{input}}{C_{reduced}}$$

A safety calculation is performed using the load advancement nuber of steps. It must always be checked wheather the final step has resulted in a fully developed failure mechanism. If that is the case the factor of safety is given by :

$$SF = \frac{available\ strength}{strength\ at\ failure} = value\ of\ \Sigma Msf\ at\ failure$$

The principle results of a safety calculation are the failure mechanism as the corresponding ΣMsf which is the safety factor.

The strength reduction methode as adopted in the safety calculation , gives similar safety factors as obtained from conventional stability analysis based on Limit Equilibrium Method (LEM) , slip circle analysis.

2.5 Cause and Mitigation of rainfall induced landslides

Rainfall infiltration significantly affects slope stability, primarily by altering the moisture content, matric suction, and shear strength of the soil within the slope. Understanding these effects is crucial for predicting and mitigating landslide risks, especially in regions prone to heavy rainfall or where slopes are already marginally stable. In unsaturated soils, matric

suction contributes to apparent cohesion, enhancing the soil's shear strength. When rainfall infiltrates the soil, it reduces matric suction as the soil becomes wetter. This reduction leads to a decrease in the apparent cohesion and overall shear strength of the soil, making the slope more susceptible to failure **[19] [20] [21]**. The loss of matric suction is particularly critical in the upper layers of the soil, where infiltration is most significant. This zone of reduced suction can propagate downward, destabilizing deeper soil layers. As rainfall infiltrates the slope, the water fills the soil pores, increasing the pore water pressure. Elevated pore water pressure reduces the effective stress in the soil, further diminishing its shear strength **[7] [9]**. In cases where the soil becomes fully saturated, the pore water pressure can approach or exceed the overburden pressure, potentially leading to soil liquefaction, especially in loose, granular soils. This condition drastically reduces the soil's shear strength, increasing the risk of slope failure **[1] [6] [19]**.

Rainfall-induced landslides pose significant hazards in many regions worldwide, necessitating the development of predictive tools to mitigate their impact. One such tool is the intensity-duration (ID) threshold curve, which identifies critical rainfall conditions that trigger landslides. The concept of rainfall thresholds for landslide initiation dates back several decades. Early studies, such as those by **Caine** (1980) **[22].** Most ID thresholds are derived empirically by analysing historical rainfall and landslide data. For instance, **Guzzetti et al.** (2007) **[23]** reviewed global rainfall thresholds and provided a comprehensive dataset from different regions, highlighting the variability in threshold values due to local geological and climatic conditions. In Japan and China, extensive studies have been conducted due to the high frequency of rainfall-induced landslides. For example, **Zhang et al.** (2019) **[25]** developed region-specific ID thresholds for southern China, accounting for monsoonal rainfall patterns. Global threshold studies, such as those by **Guzzetti et al.** (2008) **[24]**, aim to provide a generalized framework that can be adapted to regional contexts. These studies highlight the importance of local calibration to improve prediction accuracy.

Understanding the types and mechanisms of these rainfall induced landslides is crucial for hazard assessment and mitigation. Shallow Landslides typically involve the movement of a thin layer of soil and weathered material over a more stable substrate. This type of landslide often triggered by intense, short-duration rainfall that saturates the soil layer, reducing its shear

strength. **Guzzetti et al.** (2008) **[24]** Developed empirical rainfall thresholds for shallow landslide initiation. Deep-Seated Landslides Involve the movement of deep soil layers or bedrock, often affecting larger volumes of material , typically triggered by prolonged, heavy rainfall that infiltrates deeply, increasing pore water pressure and reducing slope stability. Keefer and Johnson (1983) discussed the role of prolonged rainfall in deep-seated landslide activation. Debris Flows are rapidly moving landslides composed of loose soil, rock, organic matter, and water, triggered by intense rainfall that causes slope failure, with the mobilized material flowing downslope as a slurry.

Numerous studies have evaluated the performance of sand drains in mitigating rainfall-induced landslides. The consensus is that sand drains are highly effective in enhancing slope stability, particularly in fine-grained soils prone to water retention. **Chu and Yan** (2005) conducted field studies on the use of vertical drains in slope stabilization. Their findings indicated that sand drains significantly reduced the likelihood of landslide occurrence by improving drainage and reducing pore water pressure. In regions like Kyushu at Japan, sand drains have been used extensively to stabilize slopes prone to heavy rainfall. Research by **Tsukamoto et al.** (2011) showed significant reductions in landslide incidents following the installation of sand drains, often in combination with surface drainage systems and retaining walls. The Geotechnical Engineering Office (GEO) has implemented sand drains in several landslide-prone areas. A study by Brand (1981) highlighted the success of these interventions, noting improved slope stability and reduced maintenance costs. **Chu and Yan** (2005) conducted field studies on the use of vertical drains in slope stabilization. Their findings indicated that sand drains significantly reduced the likelihood of landslide occurrence by improving drainage and reducing pore water pressure.

Mitigating these landslides involves various engineering solutions, with concrete piles being one of the most effective methods. **Chen and Wang** (2016) explore how concrete piles increase the shear resistance of slopes by providing additional support against sliding forces. **Murthy** (2002)provides a comprehensive overview of the mechanics of pile-soil interaction in stabilizing slopes. **Liu et al.** (2009) investigate the optimal spacing and depth of piles for maximum effectiveness in landslide-prone areas. **Poulos** (1995) offers guidelines for determining the appropriate embedment depth of piles based on soil characteristics and slope

geometry.**Wang et al.** (2013) present a case study of using concrete piles to stabilize slopes in urban Hong Kong, emphasizing the challenges and successes. **Ng et al.** (2001) detail the implementation of piles for slope stabilization in residential areas, highlighting the importance of site-specific design.

CHAPTER : 3

STUDY AREA , DATA AND METHOLOGY

3.1 Study Area

A fresh landslide was observed in Pangthang, East Sikkim, in 2020, which is the focus area of this study. The geographical coordinates of the location near the toe and top are 27.3727°N, 88.5838°E and 27.3724°N, 88.5841°E, respectively. During a field visit, newly constructed buildings were observed at the top of the slope. A small hilly stream, locally called Jhora or Nala, passes through this area, carrying a large amount of water after heavy precipitation **[1]**. The field photograph in **Fig. 4** shows the surcharge load from the newly constructed buildings, an anthropogenic activity, imposing a lateral load that may initiate land sliding.

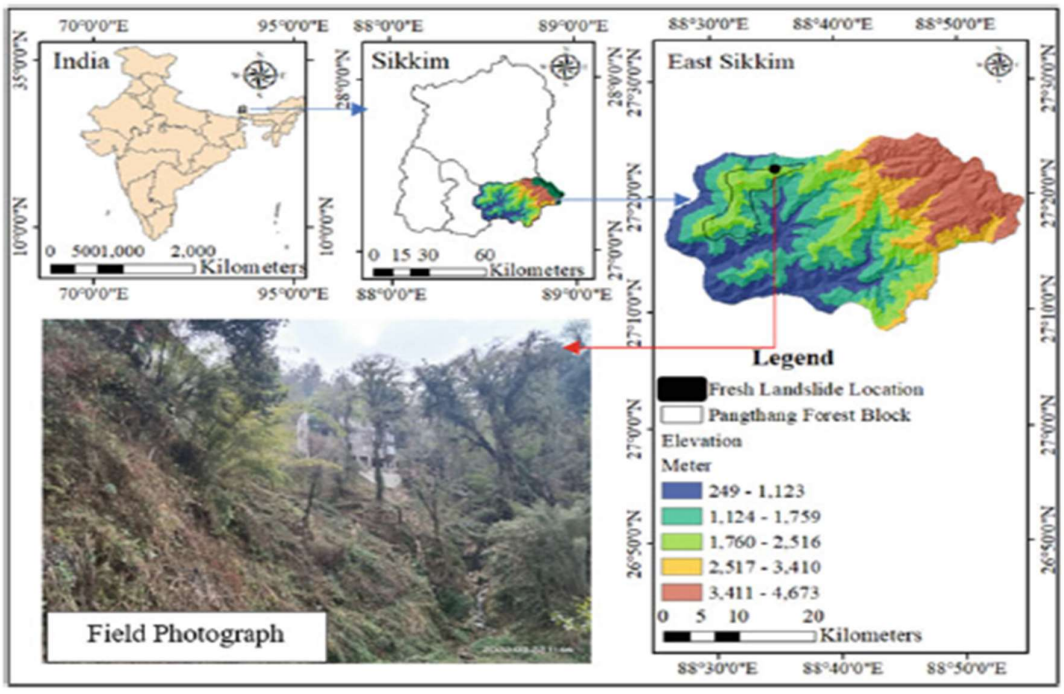

Fig.4 : Study area at pangthang, East Sikkim (Ref. – Joyita et al.**[1])**

3.2 Field Data

Joyita et al.**[1]** conducted a field visit and collected data, noting that the foundation of a recently built superstructure has become exposed. Additionally, a soil mass moved downward at another point in the middle of the slope due to the landslide. The slope under study has an inclination of 40.33° and a height of 26.00 meters. They conducted a subsoil investigation in this study area to understand the subsoil characteristics. The subsoil profile and its characteristics, as presented in **Table 1**, were found to be as follows.

There are two stratums available upto 12.0 m depth, **Stratum I**: (0.00−3.00 m) having the Organic Clay, N Value has observed as 8, having 100% water loss. The parameters of subsoil was obtained as, Grain Size Distribution: Gravel: 24%, Course Sand: 10%, Medium Sand: 22%, Fine Sand: 16%, Silty Clay: 28%; Bulk Density: 16.5 kN/m^3; NMC: 33.4%; C: 10.0 kN/ m^2; φ = 26º; and **Stratum II**: (3.00−12.00 m) having the Sandy soil with Weathered Granite Gneiss having 100% water loss. The parameters of subsoil was obtained as, Grain Size Distribution: Gravel: 24%, Course Sand: 10%, Medium Sand: 22%, Fine Sand: 16%, Silty Clay: 28%; Bulk Density: 18 kN/m^3; NMC: 21.8%; C: 0.0 kN/ m^2; φ = 35º; average N value is observed 25.

Depth (m)	Unsaturated Unit Wt. (KN/m^2)	Saturated Unit Wt. (KN/m^2)	Moisture Content (٪)	Grain Size Distribution					Shear Strength Parameters		SPT Value $(N_1)_{60}$
				Gravel	Sand			Silty Clay	C (KN/m^2)	φ (º)	
					Coarse-Sand	Medium-Sand	Fine-Sand				
0 to 3	16.5	19.5	33.4	24	10	22	16	28	10	26	8
3 to 12	18	20	21.8	30	20	26	22	2	0	35	25

Table 1 : Detail results of subsoil investigation .

Joyita et al.**[1]** conducted a trend analysis of 12 years (2009−2020) of precipitation data obtained from the Indian Meteorological Department, Government of India (IMD). Their

analysis reveals an increasing rate of untimely precipitation (**Table 2**). The monthly rainfall data for Sikkim in 2023 from the Indian Meteorological Department presented in **Table 3**.

Precipitation	2009	2020	% Increase
Average annual precipitation (mm)	190.93	237.53	24.41
Average monsoon precipitation (mm)	311.10	448.23	44.08

Table 2 : Trend of precipitation at East Sikkim, as obtained from IMD for the Period of 2009–2020

Climate change has a significant impact on precipitation patterns. As global temperatures rise, the atmosphere's capacity to hold moisture increases, leading to changes in precipitation frequency, intensity, and distribution. More intense and frequent heavy rainfall events have been observed, leading to a higher risk of flooding.

Month	January	February	March	April	May	June	July	August	September	October	November	December
Rain fall in mm	31.5	45.7	65.8	81.2	160.4	312.5	450.3	430.7	320.6	120.3	35.4	22.1

Table 3 : monthly rainfall data for Sikkim in 2023

Heavy precipitation occurred prior to the landslide, as previously mentioned. The absence of a proper drainage system allowed water to percolate through the ground. Additionally, a nearby hilly jhora overflowed, contributing to subsurface water infiltration. This infiltrated water likely increased pore water pressure. Subsoil investigations revealed that organic clay extends up to 3 meters, making the area more susceptible to increased pore water pressure, which is a significant factor in the landslide and exposure of the foundation. Beyond the influence of pore water pressure, anthropogenic activities, such as the surcharge load from constructing a superstructure, may have further accelerated the landslide.

3.3 MODELLING IN PLAXIS-2D

PLAXIS 2D is a specialized two-dimensional finite element program used for deformation, stability, and flow analysis in various geotechnical applications. Real-world situations can be modeled using either a plane strain or an axisymmetric model. The program features a conventional graphical user interface that allows users to quickly generate a geometry model and finite element mesh based on a representative vertical cross-section of the scenario being analyzed. The process of modelling the concerned problem is discussed pointwise in following paragraphs.

3.3.1 General Settings

The slope is analyzed using a plane strain model, assuming zero displacements and strains in the z-direction, while fully accounting for normal stresses in the z-direction. For modeling soil layers and volume clusters, 15-node triangular elements are selected due to their high accuracy and ability to produce high-quality stress results for complex problems. The units used for length, force, and time are meters (m), kilonewtons (kN), and hours(h), respectively. The first step in every analysis is to set the basic parameters of the finite element model in the General Settings window. These settings include several crucial component like the basic units, ensuring consistency and accuracy across measurements; and the size of the draw area, which establishes the spatial boundaries for the modeling environment. This careful setup lays the groundwork for a precise and effective simulation process. **Fig. 5** illustrates the project properties, offering a visual representation of these initial configurations and their arrangement within the software interface.

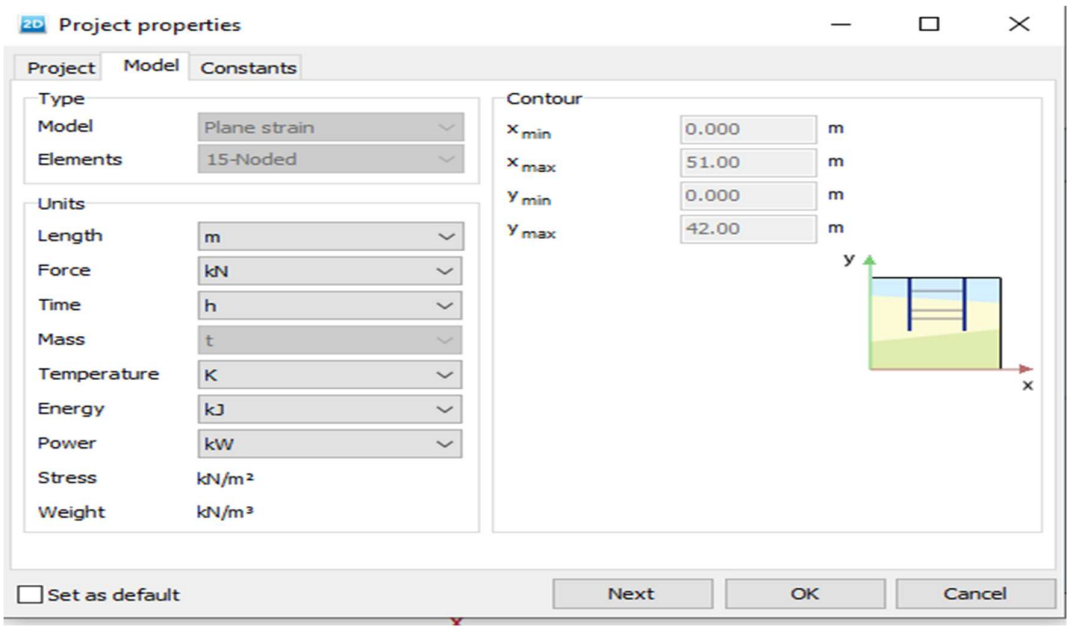

Fig. 5 : Basic Project properties

3.3.2 Geometry Model Creation

The slope geometry is established by creating two boreholes at a distance 31m, ensuring that the slope angle and soil layers were automatically set as discussed previously. Fig. 6 shows (a) slope geometry (b) borehole 1 and (c) borehole 2.

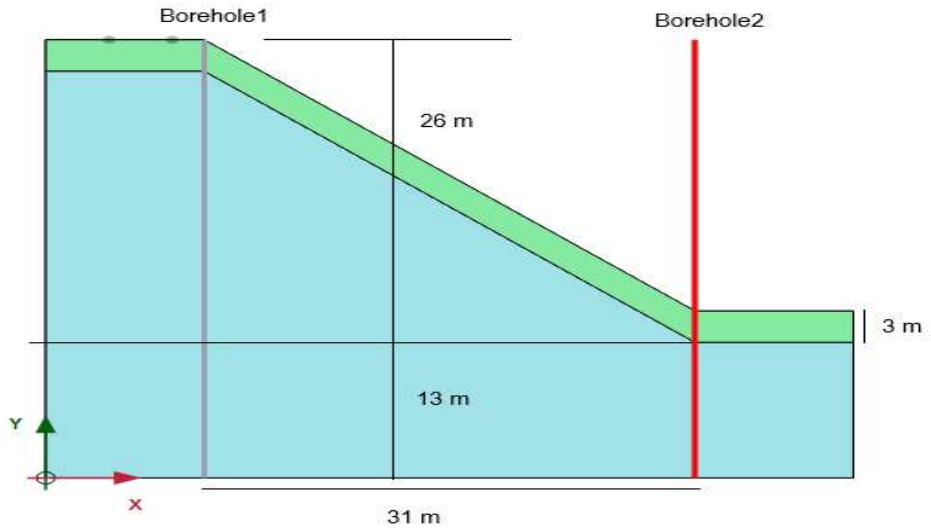

(a)

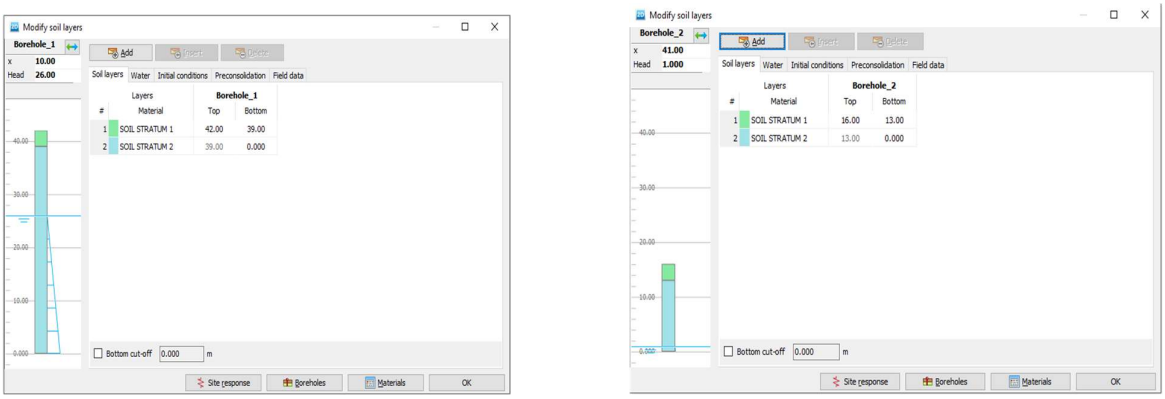

(b) (c)

Fig. 6 : (a) Geometry of slope ; (b) Borehole 1 data ; (c) Borehole 2 data

3.3.3 Material Properties Assignment and Loading Setup

Two soil materials, SOIL STRATUM 1 and SOIL STRATUM 2, are assigned according to the soil layers identified in the subsoil investigation described in the previous section. The upper layer, SOIL STRATUM 1, is composed of organic soil, while the lower layer, SOIL STRATUM 2, consists of sandy soil with weathered granite gneiss and a large percentage of gravel. Saturated and unsaturated unit weights, cohesions, and friction angles are assigned based on the field data obtained.Young's modulus of two soil type is calculated from SPT (N) value.

SOIL STRATUM 1 : E = 5000 KN/ m^2

SOIL STRATUM 2 : E = 20600 KN / m^2

For flow analysis, the permeability of the soil is required but is not present in the subsoil investigation data. However, based on the grain size distribution data from the dataset, PLAXIS evaluated the saturated permeabilities, Soil-Water Characteristic Curves (SWCC), and Hydraulic Conductivity Functions (HCF) of the two soil materials. The SWCC and HCF of the two soil materials are shown in **Fig. 7**.

Saturated permeability of SOIL STRATUM 1 : 0.1458 m/h

SOIL STRATUM 2 : 0.2970 m/h

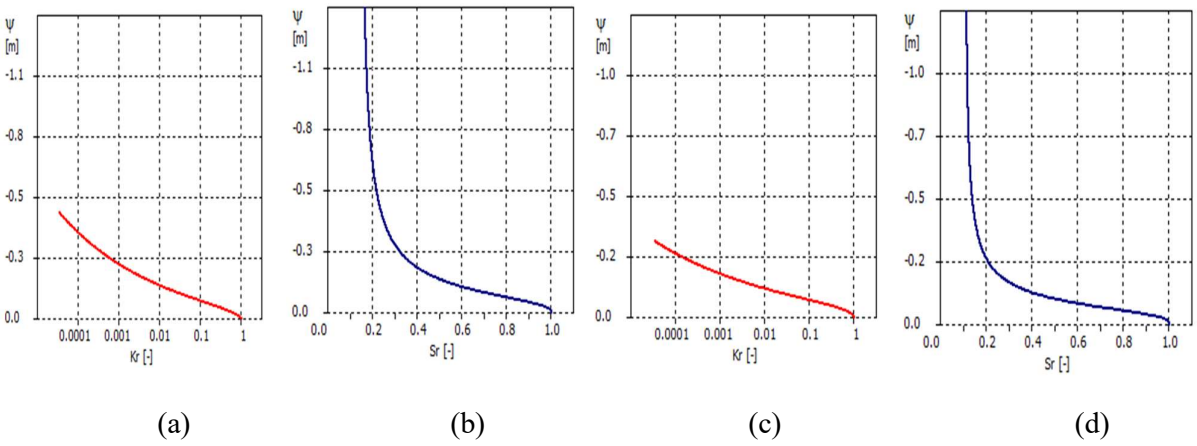

(a) (b) (c) (d)

Fig. 7 : (a) HCF (b) SWCC of SOIL STRATUM 1 ; (c) HCF (b) SWCC of SOIL STRATUM 2

To assign the building load in the model, a line load of 4 meters in length is created at the crest of the slope, positioned 2 meters from the crest point. The load intensity is 50 kN/m, as shown in **Fig. 8**. For the proposed remedial measures step ,(1) sand drains are also assigned as DRAIN; (2) concrete piles are assigned as embaded beam ROW in the model as shown in **Fig. 11.**

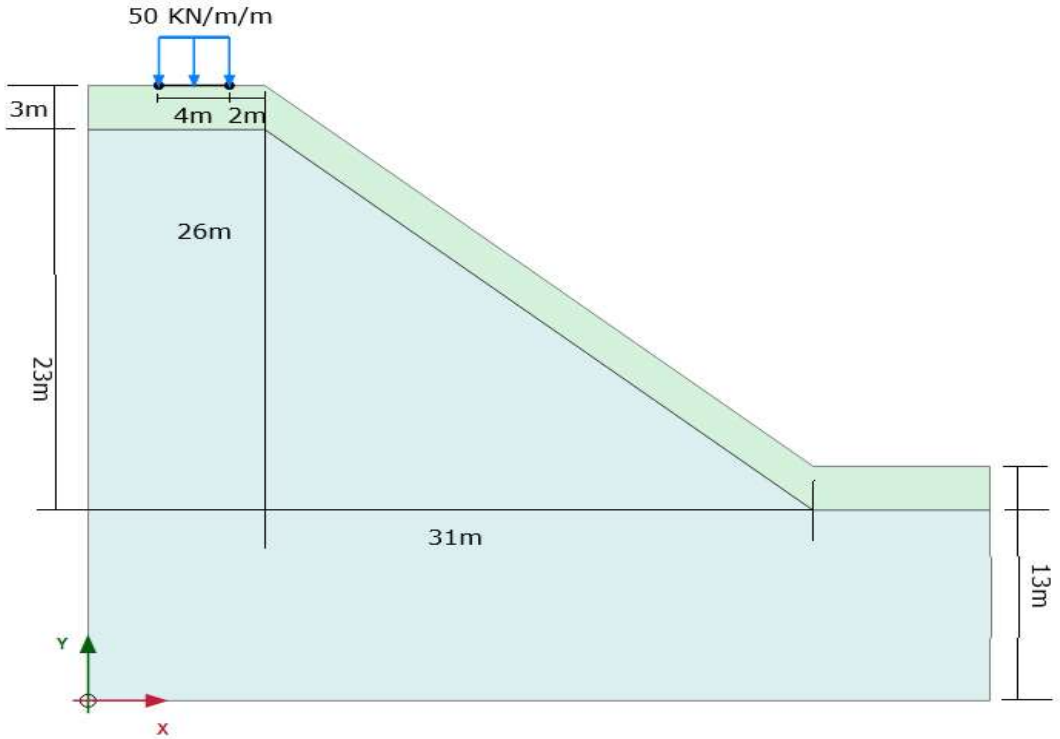

Fig. 8 : Surcharge load at model

Properties of concrete columns taken are written following:

MATERIAL TYPE :	ELASTIC
YOUNG'S MODULUS :	40* 10^6 KN/m^2
POISSON RATIO :	0.15
BEAM TYPE :	PREDEFINED
PREDEFINED BEAM TYPE :	CIRCULAR BEAM
DIAMETER :	0.150m
AXIAL SKIN RESISTANCE TYPE :	CONSTANT
AXIAL SKIN RESISTANCE VALUE :	15 KN/m^2
LATERAL RESISTANCE TYPE :	CONSTANT
LATERAL RESISTANCE VALUE :	15 KN/m^2
BASE RESISTANCE :	80 KN/m^2

3.3.4 Finite Element Mesh Generation

A fine-sized finite element mesh is created using 15-node triangular elements, which are specifically designed to enhance the accuracy and precision of the simulation as shown in **Fig. 9**. These elements, also known as quadratic triangular elements, include additional nodes that allow for a more detailed representation of the geometry and field variables. Each 15-node triangular element features three corner nodes, three mid-side nodes along each of its sides, and six internal nodes, enabling the mesh to capture complex variations within the element. This increased node count allows for better approximation of curved boundaries and more accurate interpolation of the solution field. By using a fine mesh, the computational model can resolve small-scale features and gradients more effectively, leading to higher fidelity results in the finite element analysis.

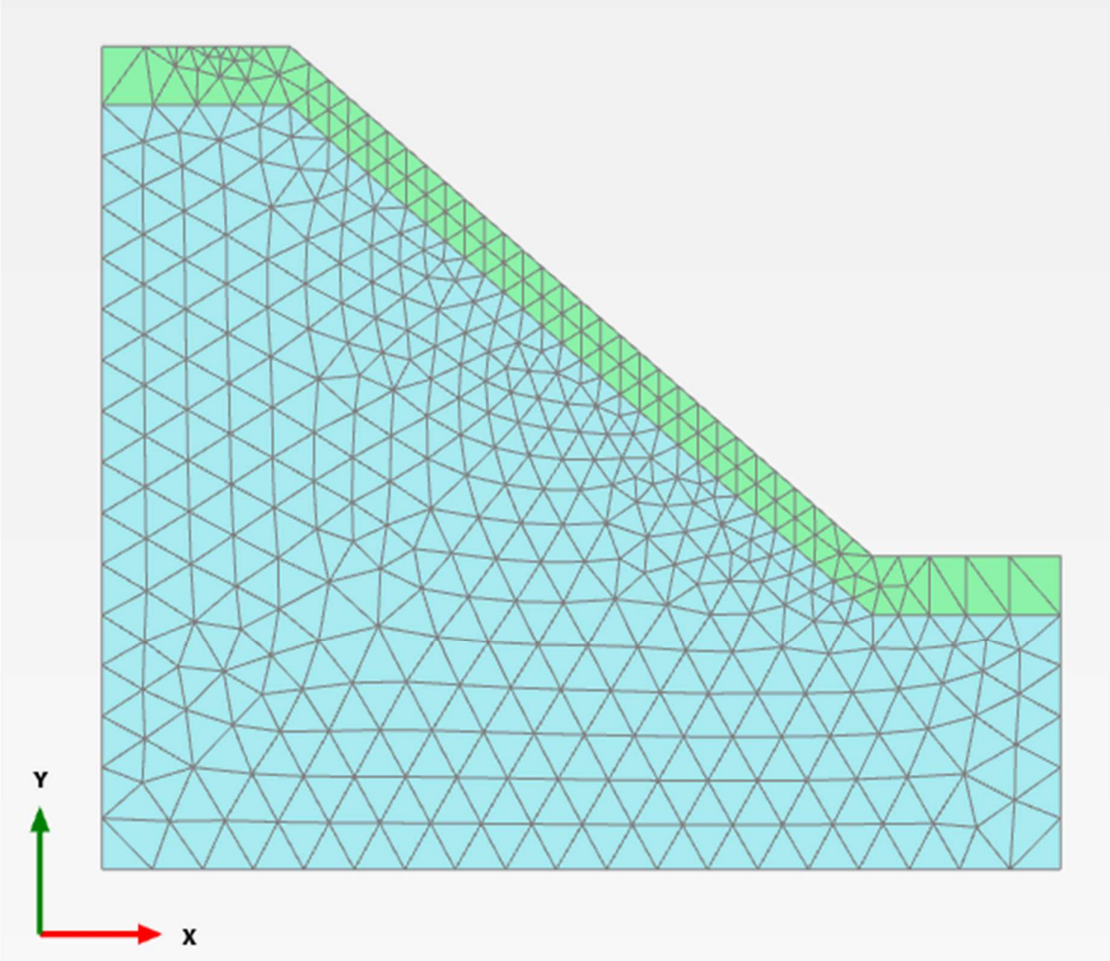

Fig. 9 : Generated Finite Eliment Mesh

3.3.5 Ground Water Flow Bounndary Conditions

For flow analysis, it's necessary to designate flow boundary conditions. The lowest boundary is assigned as closed, while side boundaries are designated as seepage boundaries. The topmost layer is set as the infiltration flow boundary condition, as illustrated in the **Fig.10**. The depth of the groundwater table isn't included in the site investigation data **[1]**, which extends to a depth of 12 meters. In this scenario, the initial groundwater table is placed at a depth of 13 meters, parallel to the slope inclination, as depicted in the **Fig.10**.

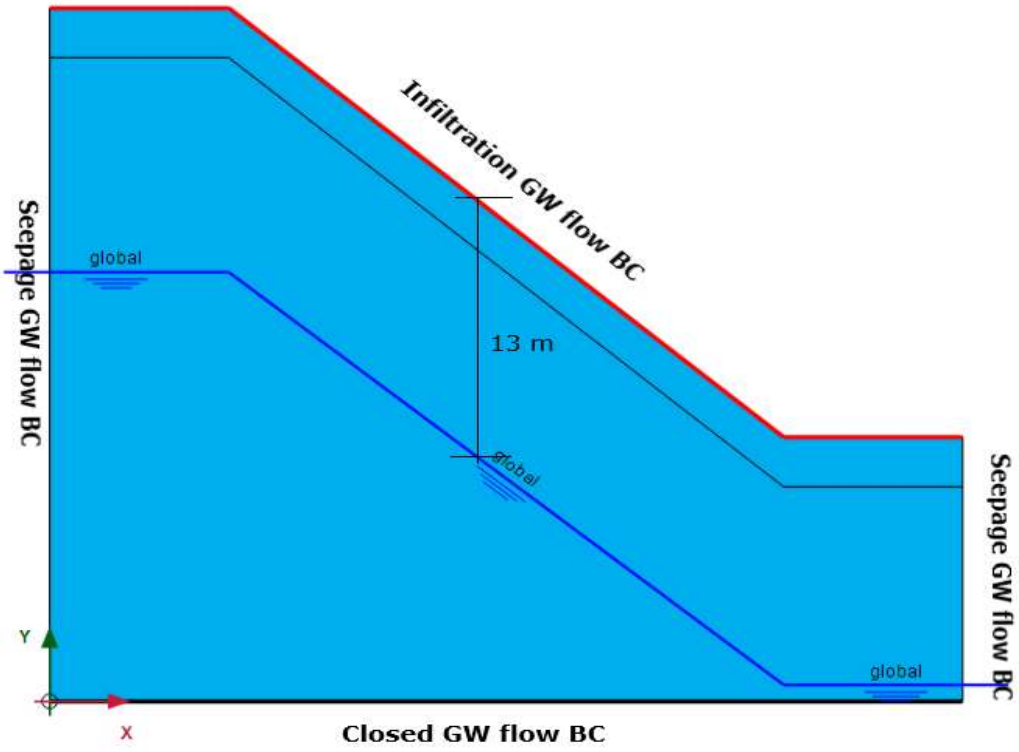

Fig.10 : Ground water table and flow bondary conditions.

When the soil is only partially saturated, determining the amount of water that can infiltrate into the soil becomes a question. The amount of water that can infiltrate into an unsaturated slope depends on various factors such as the slope's soil type, porosity, permeability, vegetation cover, rainfall intensity, and duration. The Horton equation is a widely used empirical model for estimating infiltration capacity, which is the maximum rate at which water can infiltrate into soil. It describes the process of infiltration as a decreasing function of time during a rainfall event. The equation states that the infiltration capacity starts at an initial rate f_0 and gradually decreases over time until it reaches a steady-state value fc. The rate of decrease is controlled by the decay coefficient k.

$$f(t) = f_c + (f_0 - f_c) \times e^{-kt}$$

Sikkim is a rainfall prone area. The intensity of rainfall has increased due to the effect of climate change. The upper soil layer of the study area is an organic clay soil with a saturated permeability of 0.1458 m/h. In this study, the rainfall infiltration capacity is assumed to be between half of saturated permeability and saturated permeability. Rainfall infiltration duration

is assumed to be 3 h in all cases and infiltration rate is taken increasing way 0.08 m/h , 0.10 m/h , 0.12 m/h in concerned analysis steps.

3.3.6 Analysis Phases

In first phase (Initial Phase) Gravity loading calculation is done . After calculation is done with Line load with intensity 50 KN/m/m . Then rain fall infiltration three phases are analyse with fully coupled deformation calculation with duration 3 hour . after all phases a safety calculation is done with safety phase separately. At last a analysis is done for proposed remidial following with a safety phase also which is described in next chapter .All cases analysed in this study is written following:

CASE 1 **:** Natural slope condition without building load and without rainfall infiltration.

CASE 2 **:** Slope with Building load (Line load with intensity 50 KN/m/m).

CASE 3 **:** Slope with Rainfall infiltration (Infiltration rate 0.08 m/h).

CASE 4 **:** Slope with Rainfall infiltration (Infiltration rate 0.10 m/h).

CASE 5 **:** Slope with Rainfall infiltration (Infiltration rate 0.12 m/h).

CASE 6 **:** Slope with building load (Load intensity 50 KN/m/m) and with rainfall Infiltration (0.12 m/h) with Proposed remedial mesures.

CHAPTER : 4

PROPOSED REMEDIAL MEASURES

The remedial measure involves two directions, as illustrated in Fig. 11, which are detailed below:

1. An attempt has been made to decrease the pore water pressure, resulting in a proposed solution to install a sand drain at 2.0m center to center in the slope direction and 1.0m center to center in the stretch direction, to a depth of 3.00 meters.This depth is limited by the presence of the weathered granite gneiss layer starting at that point which is more permeable than upper layer. To reduce the pore water pressure, it has been recommended to use the sand drain to subsurface pore water pressure and discharge it at more permeable second leayer. Pore water pressure decrease means effective stress increase and stability of slope increase.

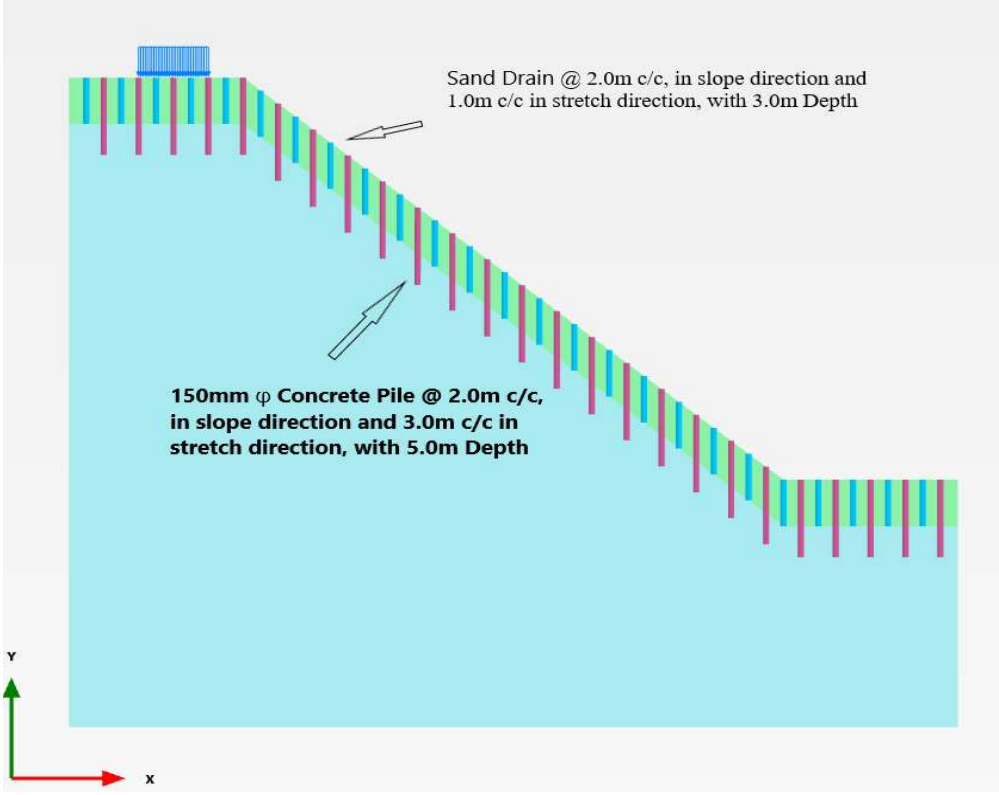

Fig. 11: Proposed remedial measures

2. The slope has been reinforced using concrete piles with a diameter of 150 mm and a length of 5.00 m, spaced at 2.0m centers in the slope direction and 3.0m centers in the stretch direction. This reinforcement increases the shear strength of the weaker upper soil layer. Additionally, the piling operation may enhance the strength of the existing soil strata through compaction. This reinforcement is also effective in retaining the soil against lateral loading, thereby restraining the lateral thrust caused by anthropogenic activities such as the construction of superstructures.

CHAPTER : 5

RESULTS AND DISCUSSIONS

CASES	Factor of Safety
CASE 1 **:** Natural slope condition without building load and without rainfall infiltration.	1.331
CASE 2 **:** Slope with Building load (Line load with intensity 50 KN/m/m).	1.284
CASE 3 **:** Slope with Rainfall infiltration (Infiltration rate 0.08 m/h).	1.117
CASE 4 **:** Slope with Rainfall infiltration (Infiltration rate 0.10 m/h).	1.028
CASE 5 **:** Slope with Rainfall infiltration (Infiltration rate 0.12 m/h).	0.950
CASE 6 **:** Slope with building load (Load intensity 50 KN/m/m) and with rainfall Infiltration (0.12 m/h) with Proposed remedial mesures.	1.450

Table 4 : Factor of Safety obtained for all cases analysed.

1 . Under fair weather conditions, the Factor of Safety become more than 1.3. Specifically, the calculated value was 1.39 (**Fig. 12**). Therefore, it can be concluded that, in fair weather conditions, the existing slope at Pangthang, East Sikkim, appears to be sufficiently stable.

2 . After applying a surcharge load of 50 kN/m² at the crest of the slope, the Factor of Safety value decreased to 1.284 (**Fig. 13**). This indicates a slight reduction in the Factor of Safety.

Notably, the surcharge load value considered is significantly higher than that of a typical building load. Therefore, it can be concluded that such a high surcharge load has a relatively minor effect on the potential for a landslide. This observation suggests that the slope maintains a considerable degree of stability even under substantial additional loading .

CASES	Maximim Pore water Pressure in KN/m^2
CASE 1 **:** Natural slope condition without building load and without rainfall infiltration.	-0.87
CASE 3 **:** Slope with Rainfall infiltration (Infiltration rate 0.08 m/h).	0.01
CASE 4 **:** Slope with Rainfall infiltration (Infiltration rate 0.10 m/h).	0.57
CASE 5 **:** Slope with Rainfall infiltration (Infiltration rate 0.12 m/h).	1.26

Table 5 : Maximum pore water pressure in all cases analysed

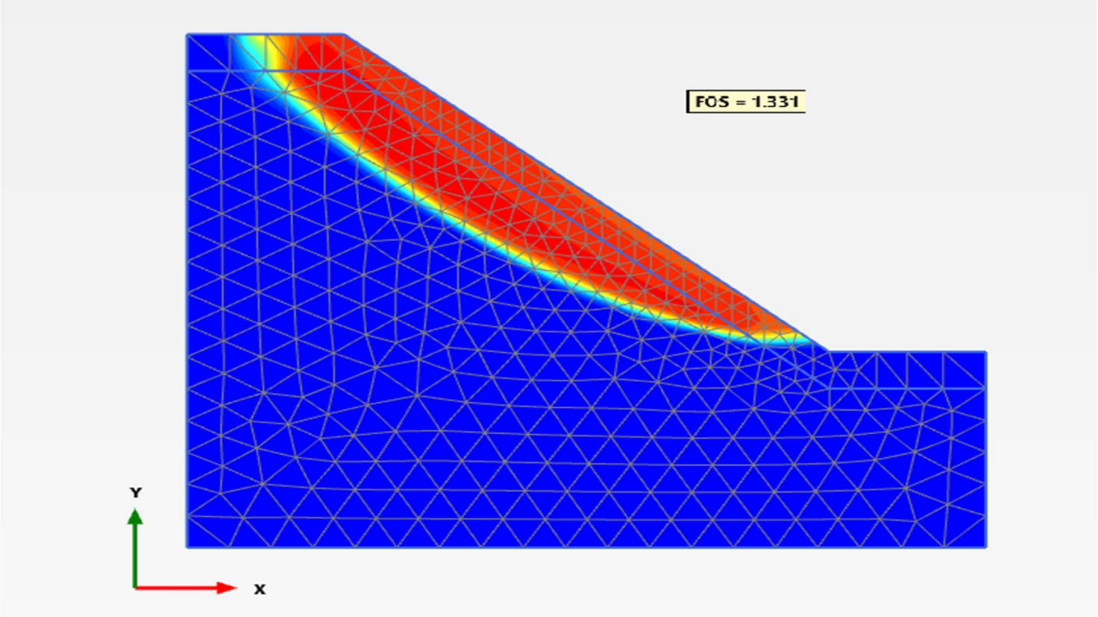

Fig. 12 : Failure surface of the slope without rainfall infiltration and surcharge load

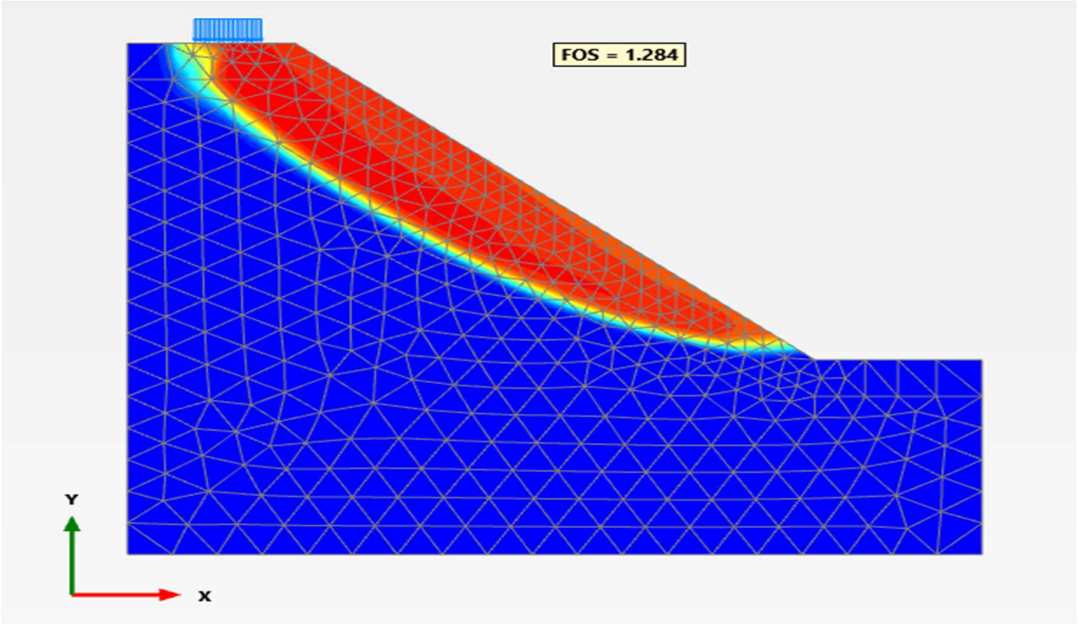

Fig. 13 : Failure surface of the slope with surcharge load but without rainfall infiltration

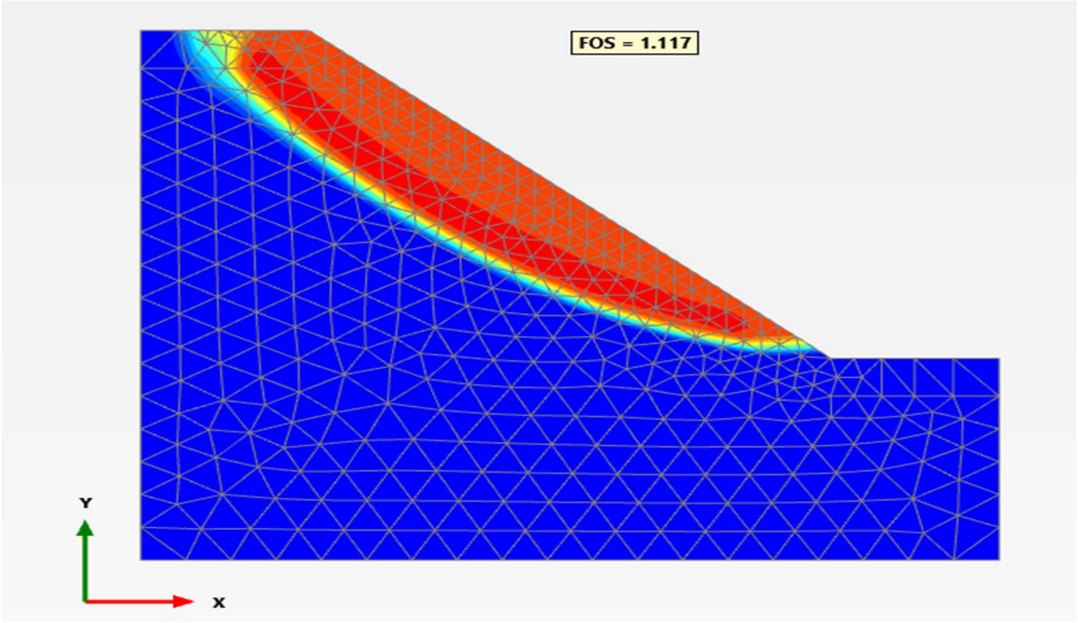

Fig . 14 : Failure surface of the slope with rainfall infiltration rate 0.08 m/h

3 . However, when we allow rainfall infiltration into the slope, the Factor of Safety value decreases more significantly. As the infiltration rate increases, the reduction in the Factor of Safety becomes more pronounced, as clearly seen from Table 4. For rainfall infiltration rates of 0.8 m/h, 0.10 m/h, and 0.12 m/h, the Factor of Safety values are 1.116, 1.028, and 0.950,

respectively. After considering the effect of a higher infiltration rate, which corresponds to higher precipitation, the Factor of Safety is reduced to 0.95 (**Fig .13** ; **Fig. 14** ; **Fig. 15**). This indicates a high risk of slope failure. In fact, slope failure occurred in the field even before reaching the maximum infiltration capacity, which is the saturated permeability of the soil. This observation underscores the significant impact of rainfall infiltration on slope stability.

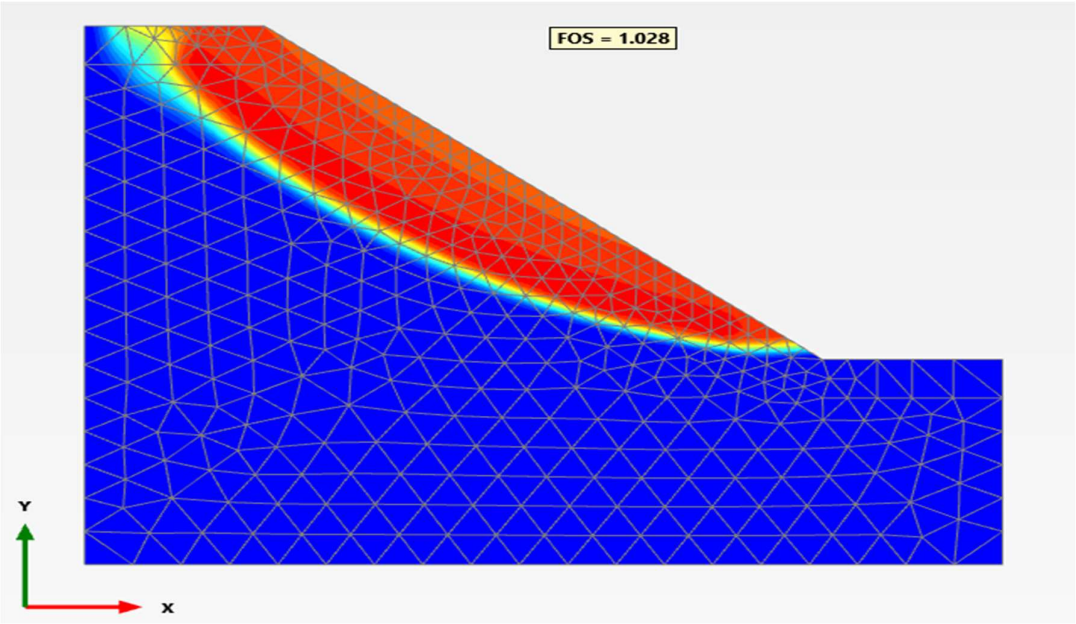

Fig. 15 : Failure surface of the slope with rainfall infiltration rate 0.10 m/h

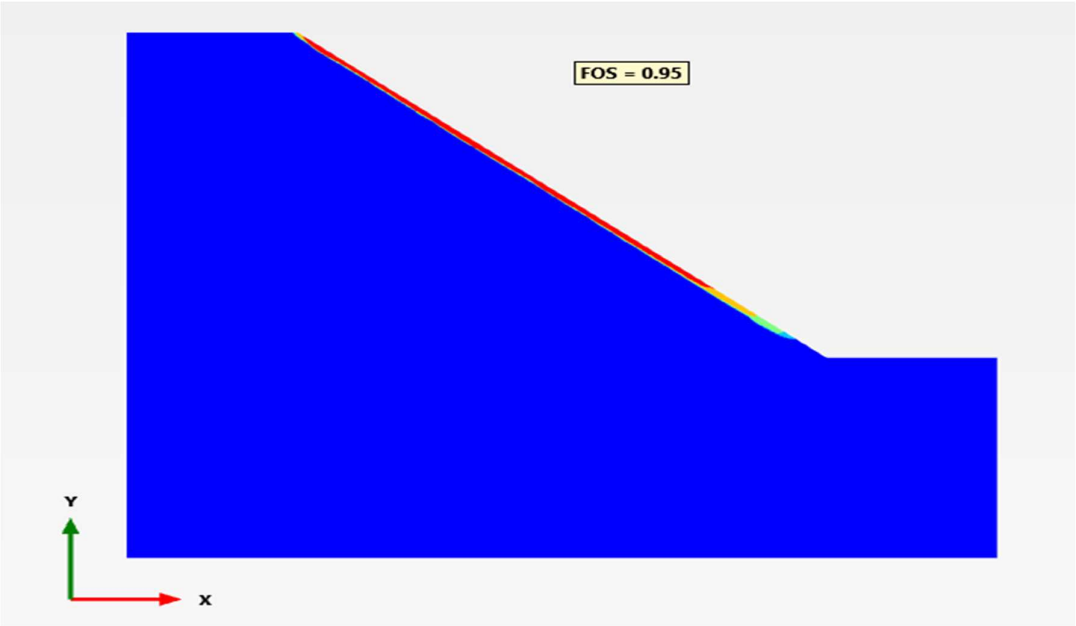

Fig. 16 : Failure surface of the slope when slope is failed (Infiltration rate 0.12 m/h)

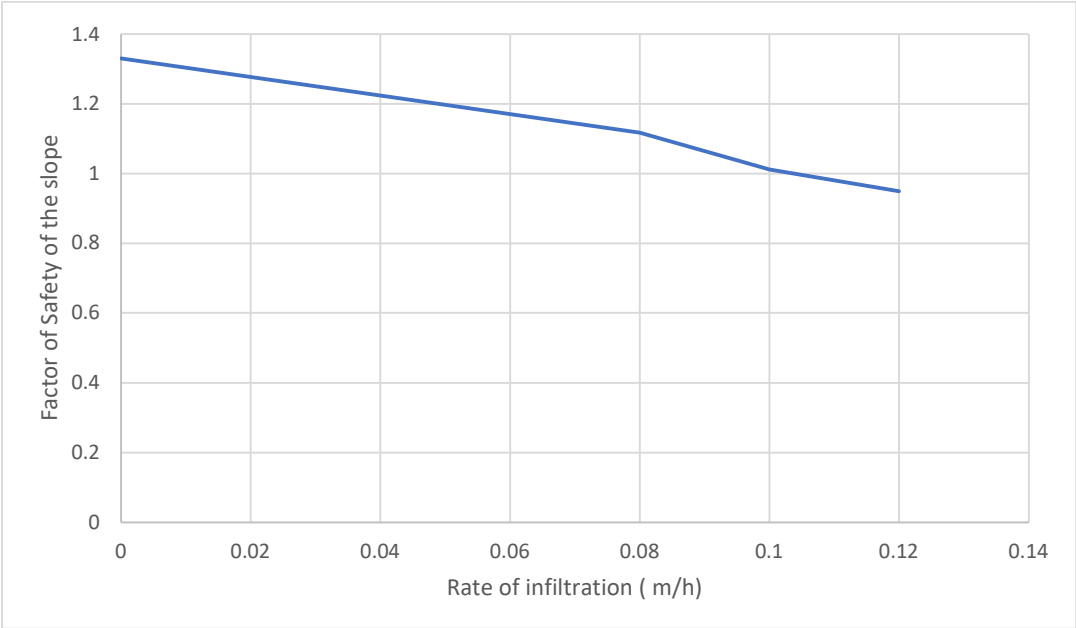

Fig. 17 : Factor of safety VS rainfall infiltration rate graph

4. A graph is plotted between the obtained factor of safety and the rainfall infiltration rate, as shown in **Fig. 16**. It clearly shows that as the infiltration rate increases, the factor of safety decreases.

5. A point below the slope surface was selected, and the pore water pressure at that point was obtained, as shown in Table 5. It was observed that as the rate of infiltration increases, the pore water pressure also increases. In Case 5(Infiltration rate is 0.12 m/h), when failure occurs, the pore water pressure reaches its maximum value. This indicates that pore water pressure is the primary culprit for the landslide.

6. As clearly seen from Table 5 in Case 1, which represents the natural condition, the pore water pressure values are negative. This indicates the presence of soil suction. Soil suction contributes to the overall shear strength of the soil by providing a form of pseudo cohesion. However, as rainwater infiltrates the soil, the suction diminishes. This reduction in suction leads to a decrease in shear strength, which consequently lowers the factor of safety.

7 . **Fig. 15** clearly shows that the failure surface emerged when the Factor of Safety dropped below 1.0, indicating a slope failure. The observed failure pattern is shallow, suggesting that the upper layers of the slope are particularly vulnerable under conditions of reduced stability. This shallow failure highlights the importance of surface stability measures and the potential

need for reinforcement or improved drainage solutions to prevent such failures, especially in scenarios involving heavy rainfall or significant infiltration events.

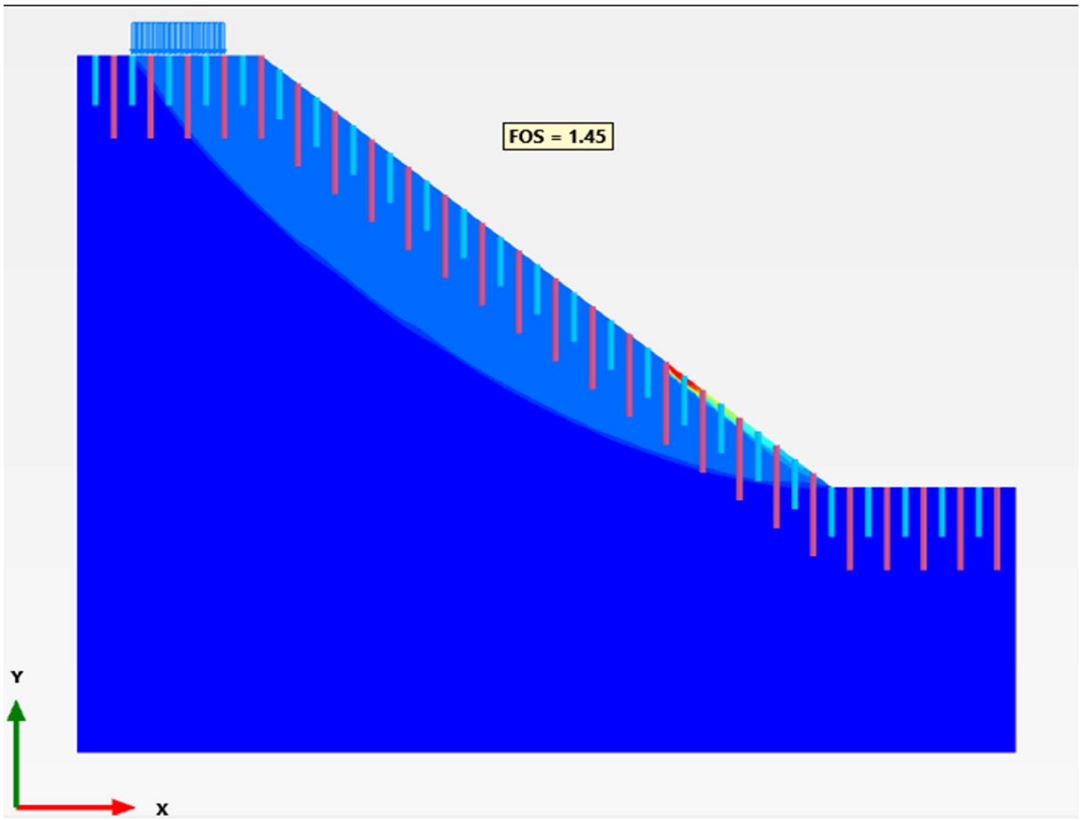

Fig. 18 : Failure surface of the slope with most adverse condition and with all remedial measures applied .

8 . Following the implementation of the remedial measures outlined in Chapter 4, the slope now demonstrates improved stability, with the Factor of Safety rising to 1.45. The concrete piles has effectively increased the shear strength of soil mass, and the installation of sand drains has successfully disipated pore water pressure. These interventions have significantly strengthened the Factor of Safety,as shown in **Fig 17** highlighting their effectiveness in enhancing slope stability. These improvements imply that the slope is now better equipped to withstand additional loads and infiltration, reducing the risk of failure and enhancing safety for the surrounding area.

CHAPTER : 6

CONCLUSIONS AND FUTURE SCOPE

The study may be summarized and concluded as follows:

This study concentrated on a landslide within a hilly terrain. Subsoil investigation data were gathered, and an examination of various factors contributing to landslides was conducted. Stability analysis of the slope was performed using the finite element-based PLAXIS 2D software. It was determined that prior to the construction of superstructures, the slope remained stable under fair weather conditions and Factor of safety obtained 1.331. The existing slope, including the additional load from the construction of superstructures imposing surcharge loads, was observed to maintain stability during fair weather conditions, with a Factor of Safety of 1.284.

But after heavy precipitation landslides occurred, a foundation of a building was exposed. A Jhora present just besides the building, and just beside the Jhora at the middle of the slope, it became fail. The stability analysis, by PLAXIS 2D software in consideration with the impact of high infiltration rate of 0.12m/h, the Factor of Safety was obtained as 0.95.

Due to heavy precipitation, subsurface flow begins, leading to the development of pore water pressure, which is the primary cause of the landslide. The observed failure pattern is shallow, indicating that the upper layers of the slope are particularly vulnerable under conditions of reduced stability. In the natural condition, the pore water pressure values are negative, signifying the presence of soil suction. Soil suction enhances the overall shear strength of the soil by providing a form of pseudo cohesion. However, as rainwater infiltrates the soil, the suction diminishes. This reduction in suction leads to a decrease in shear strength, consequently lowering the factor of safety.

The proposed solution involves installing sand drains at specific intervals within the slope to reduce pore water pressure. The drains are suggested to be placed 2.0 meters apart in the slope direction and 1.0 meter apart in the stretch direction, reaching a depth of 3.00 meters. The depth is limited by the presence of a more permeable weathered granite gneiss layer. These drains aim to alleviate pore water pressure by directing it to the more permeable layer below,

leading to increased effective stress and improved slope stability. The slope has been reinforced using concrete piles with a diameter of 150 mm and a length of 5.00 m, spaced at 2.0m centers in the slope direction and 3.0m centers in the stretch direction. This reinforcement increases the shear strength of the weaker upper soil layer.

After providing the remedial measures the slopes become completely stable, with a Factor of Safety 1.45. The likelihood of future landslides has diminished; nevertheless, regular observation and maintenance have become imperative.

REFERENCES

1. Golder, J., Halder, S., & Bhandari, G. (2023). Impact of Heavy Precipitation on Landslide Due to Climate Change and Probable Remedial Measure. (S. Mitra , K. Dasgupta, A. Dey, & A. Bedamatta, Eds.) *Disaster Management and Risk Reduction: Multidisciplinary Perspectives and Approaches in the Indian Context*, 61-80. doi:10.1007/978-981-99-6395-9_4

2. Bishop, A. W. (1955). The use of the Slip Circle in the Stability Analysis of Slopes. *First Technical Session : General Theory of Stability of Slopes*. doi:https://doi.org/10.1680/geot.1955.5.1.7

3. Dawson, E. M., Roth, W. H., & Drescher, A. (1999, December). Slope stability analysis by strength reduction. *Geotechnique, 49*, 835-840. doi:https://doi.org/10.1680/geot.1999.49.6.835

4. Zienkiewicz, O. C., Humpheson, C., & Lewis, R. W. (1975). Associated and non-associated visco-plasticity and plasticity in soil mechanics. *Geotechnique, 25*, 671-689. doi:https://doi.org/10.1680/geot.1975.25.4.671

5. Griffiths, D. V., & Lane, P. A. (1999, June). Slope stability analysis by finite elements. *Geotechnique, 49*(3), 387-403. doi:https://doi.org/10.1680/geot.1999.49.3.387

6. Chatra, A., & Dodagoudar, G. R. (2017). Numerical modelling of rainfall effects on the stability of soil slopes. *International Journal of Geotechnical Engineering*, 425-437. doi:https://doi.org/10.1080/19386362.2017.1359912

7. Onyango, J. A., & Chunyang, Z. (2019, June). *Environmental and Earth Sciences Research Journal, 6*, 89-96. doi:https://doi.org/10.18280/eesrj.060206

8. Jacob, A., Thomas, A. A., Nath, A. G., & MP, A. (2018). SLOPE STABILITY ANALYSIS USING PLAXIS 2D. *International Research Journal of Engineering and Technology (IRJET), 6*, 3366-3368.

9. Wu, L. Z., Huang, R. Q., Xu, Q., Zhang, L. M., & Li, H. L. (2015, January 7). Analysis of physical testing of rainfall-induced soil slope failures. *Environmental Earth Science, 73*, 8519-8531. doi:DOI 10.1007/s12665-014-4009-8

10. Prodan, M. V., Peranić, J., Pajalić, S., & Arbanas, Ž. (2023). Physical Modelling of Rainfall-Induced Sandy and Clay-Like Slope Failures. *Advances in Materials Science and Engineering, 2023*, 12. doi:10.1155/2023/3234542

11. Fayaz, P. H., & Chalotra, S. (2022). Physical Modeling of Rainfall and Induced Landslide. *International Journal of Innovative Research in Engineering & Management (IJIREM), 9*(2), 121-126. doi:10.55524/ijirem.2022.9.2.15

12. Wang, S., Idinger, G. & Wu, W. Centrifuge modelling of rainfall-induced slope failure in variably saturated soil. *Acta Geotech.* **16**, 2899–2916 (2021). doi:10.1007/s11440-021-01169-x

13. Zhai, Q., & Rahardjo, H. (2015, December). Estimation of permeability function from the soil–water characteristic curve. *Engineering Geology, 199*, 148-156. doi:10.1016/j.enggeo.2015.11.001

14. Bishop, A. W., & Blight, G. E. (1963). SOME ASPECTS OF EFFECTIVE STRESS IN SATURATED AND PARTLY SATURATED SOILS. *Géotechnique, 13*(3), 177-197. doi:10.1680/geot.1963.13.3.177

15. Fredlund, D. G., Morgenstern, N. R., & Widger, R. A. (1978, August). The shear strength of unsaturated soils. *Canadian Geotechnical Journal, 15*(3). doi:10.1139/t78-029

16. Fredlund, D. G., Xing, A., Fredlund, M. D., & Barbour, S. L. (1996). The relationship of the unsaturated soil shear strength to the soil-water characteristic curve. *Canadian geotechnical journal*, *33*(3), 440-448.

17. Aqib, M., Usmani, S., Khan, T., Sadique, M. R., & Alam, M. M. (2023). Experimental and numerical analysis of rainfall-induced slope failure of railway embankment of semi high-speed trains. Journal of Engineering and Applied Science, 70(1).doi:10.1186/s44147-023-00188-7

18. Mburu, J. W., Li, A. J., Lin, H. D., & Lu, C. W. (2022). Investigations of Unsaturated Slopes Subjected to Rainfall Infiltration Using Numerical Approaches—A Parametric Study and Comparative Review. *Sustainability*, *14*(21), 14465. https://doi.org/10.3390/su142114465

19. Chen, L., & Young, M. H. (2006). Green-Ampt infiltration model for sloping surfaces. *Water Resources Research*, *42*(7). https://doi.org/10.1029/2005wr004468

20. Ng, C. W. W., & Shi, Q. (1998). A numerical investigation of the stability of unsaturated soil slopes subjected to transient seepage. *Computers and geotechnics*, *22*(1), 1-28. 10.1016/S0266-352X(97)00036-0
21. Zhan, T. L., & Ng, C. W. (2004). Analytical analysis of rainfall infiltration mechanism in unsaturated soils. *International Journal of Geomechanics*, *4*(4), 273-284. 10.1061/(ASCE)1532-3641(2004)4:4(273)
22. Caine, N. (1980). The Rainfall Intensity - Duration Control of Shallow Landslides and Debris Flows. *Geografiska Annaler: Series A, Physical Geography*, *62*(1–2), 23–27. https://doi.org/10.1080/04353676.1980.11879996
23. Guzzetti, F., Peruccacci, S., Rossi, M. *et al.* The rainfall intensity–duration control of shallow landslides and debris flows: an update. *Landslides* **5**, 3–17 (2008). https://doi.org/10.1007/s10346-007-0112-1
24. Guzzetti, F., Ardizzone, F., Cardinali, M., Galli, M., Reichenbach, P., & Rossi, M. (2008). Distribution of landslides in the Upper Tiber River basin, central Italy. *Geomorphology*, *96*(1–2), 105–122. https://doi.org/10.1016/j.geomorph.2007.07.015
25. Zhang, S., Xu, C., Wei, F., Hu, K., Xu, H., Zhao, L., & Zhang, G. (2020). A physics-based model to derive rainfall intensity-duration threshold for debris flow. *Geomorphology*, *351*, 106930. https://doi.org/10.1016/j.geomorph.2019.106930